Technical University of Denmark

Determination of radioisotopes using ICPMS

Roos, Per

Publication date:
2013

Citation (APA):
Roos, P. (2013). Determination of radioisotopes using ICPMS [Sound/Visual production (digital)]. NKS Workshop on Radioanalytical Chemistry, Roskilde, Denmark, 02/09/2013, http://www.nks.org/en/seminars/presentations/nks-b_radioanalysis_workshop_2-6_september_2013.htm

Determination of radioisotopes using ICP-MS

The coupling between chemistry and instrumentation.

Per Roos
DTU NUTECH

Use of ICP-MS in analysing radioisotopes

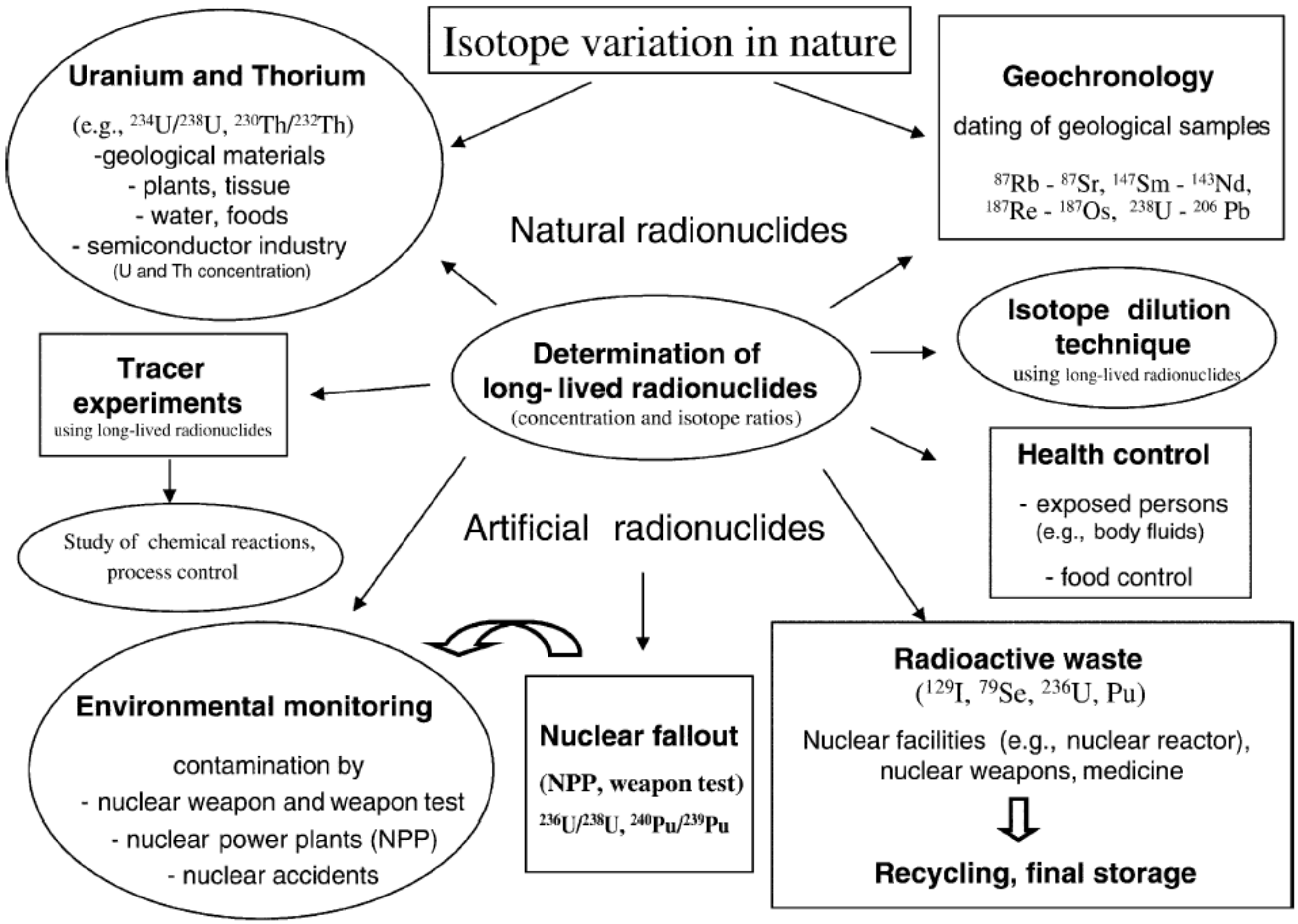

Fig. 1. Overview of application fields for determination of long-lived radionuclides.

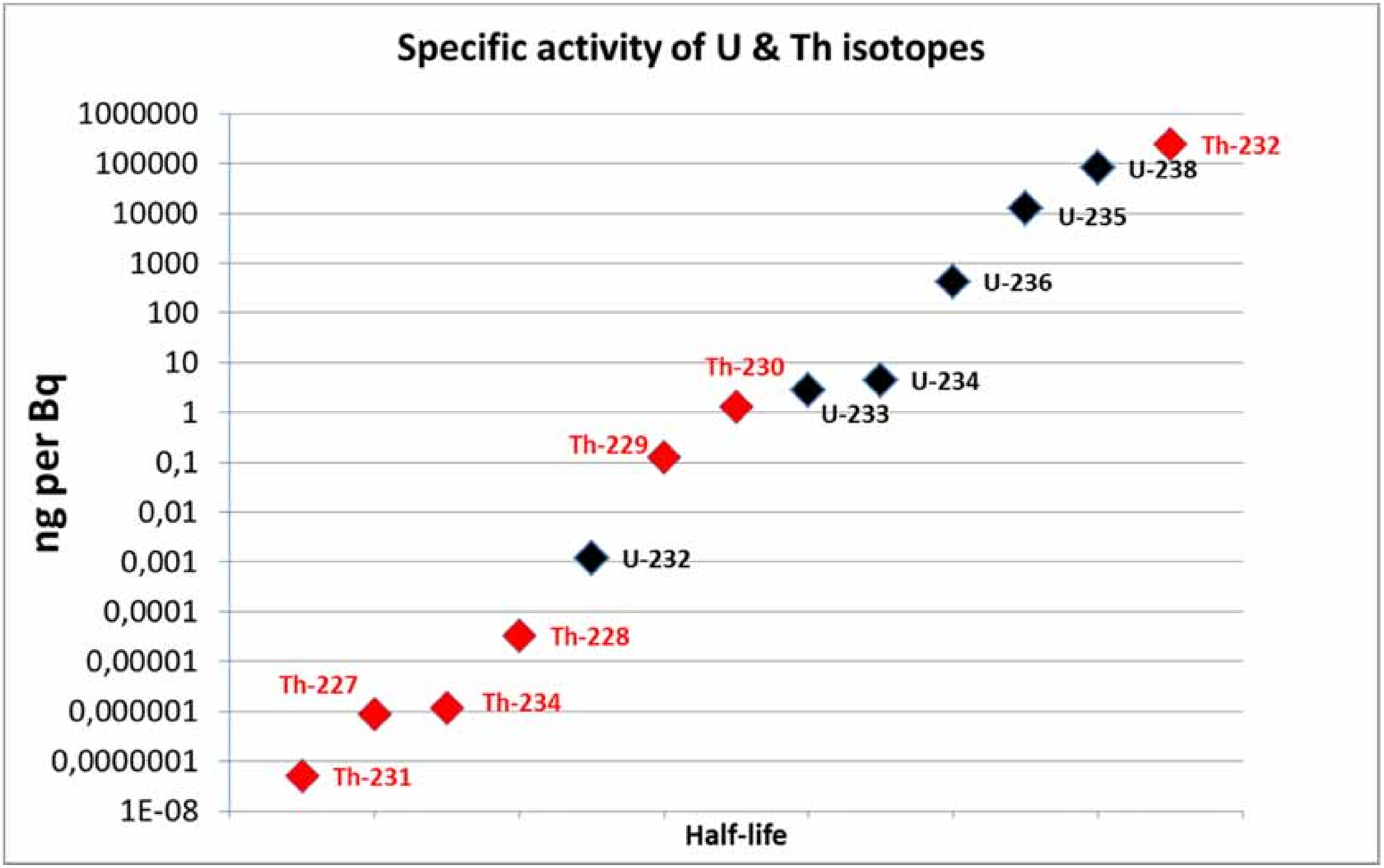

Specific activity of U & Th isotopes
ng per Bq
Half-life
1000000
100000
10000
1000
100
10
1
0,1
0,01
0,001
0,0001
0,00001
0,000001
0,0000001
1E-08
Th-232
U-238
U-235
U-236
Th-230
U-234
U-233
Th-229
U-232
Th-228
Th-227
Th-234
Th-231

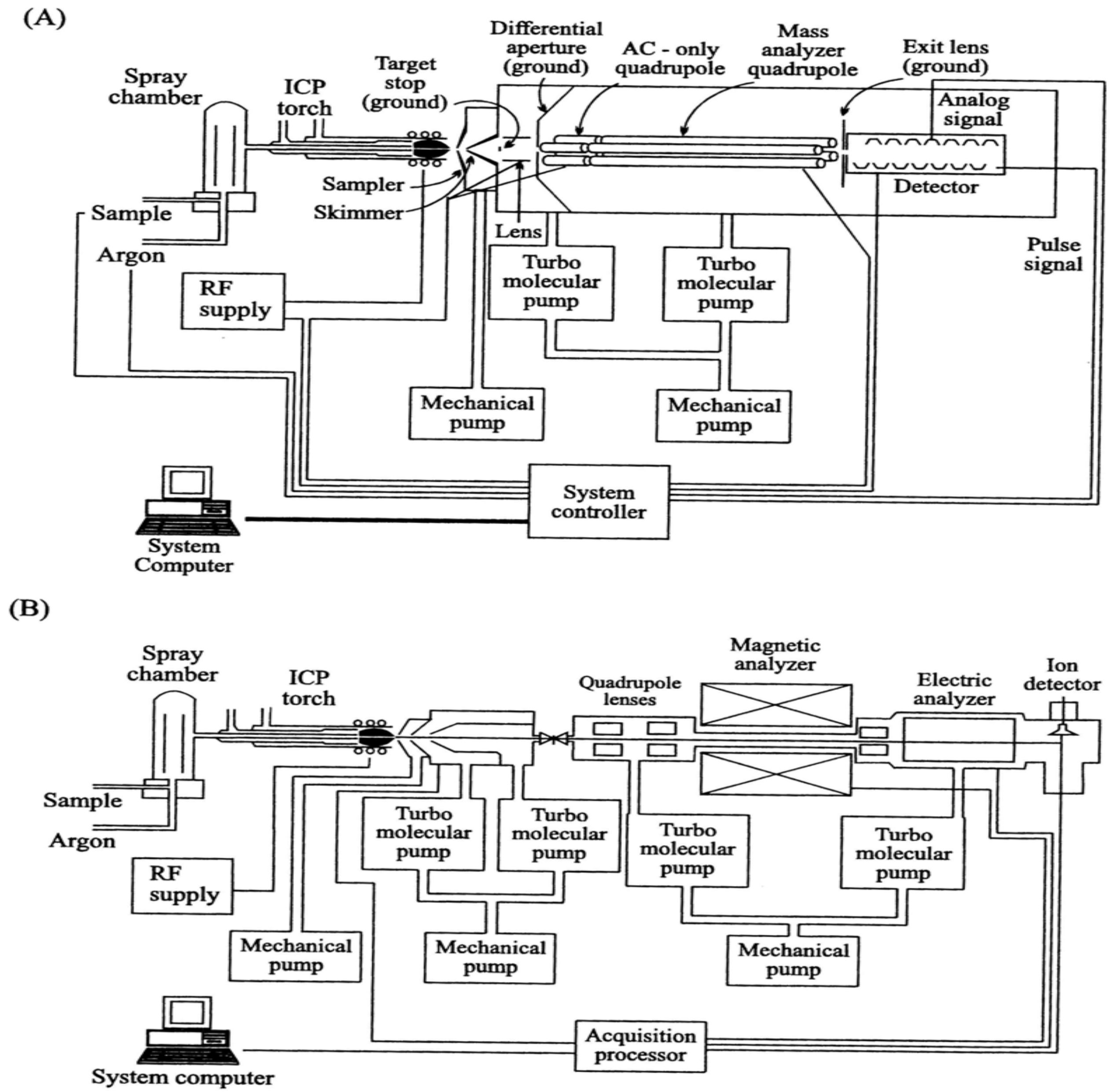

Figure 1.4 (A) Schematic diagram of a quadrupole ICPMS, the Elan 6000. (Courtesy of the Perkin-Elmer/Sciex Corporation.) (B) Schematic diagram of a magnetic sector ICPMS, the JMS-PLASMAX2. (Courtesy of JOEL Incorporated.)

Plasma Trace II – High resolution ICP-MS

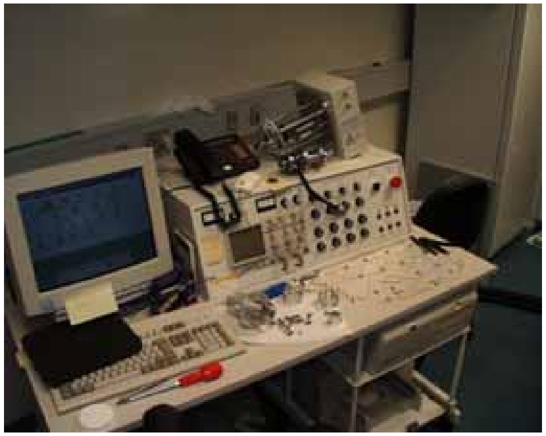

Thermo X-series II – Quadrupole ICP-MS

Table 1.3 Distribution of ionization energies among the elements for singly and doubly charged ions. Grouped in steps of 1 eV.

Ionization Energy (eV)	Elements	2^+ *Ions*
<7	Li, Na, Al, K, Ca, Sc, Ti, V, Cr, Ga, Rb, Sr, Y, Zr, Nb, In, Cs, Ba, La, Ce, Pr, Nd, Pm Sm, Eu, Gd, Tb, Dy, Ho, Er, Tm, Yb, Lu, Hf, Tl, Ra, Ac, Th, U	
7–8	Mg, Mn, Fe, Co, Ni, Cu, Ge, Mo, Tc, Ru, Rh, Ag, Sn, Sb, Ta, W, Re, Pb, Bi	
8–9	B, Si, Pd, Cd, Os, Ir, Pt, Po	
9–10	Be, Zn, As, Se, Te, Au	
10–11	P, S, I, Hg, Rn	Ba, Ce, Pr, Nd, Ra
11–12	C, Br	Ca, Sr, La, Sm, Eu, Tb, Dy, Ho, Er
12–13	Xe	Sc, Y, Gd, Tm, Yb, Th, U, Ac
13–14	H, O, Cl, Kr	Ti, Zr, Lu
14–15	N	V, Nb, Hf
15–16	Ar	Mg, Mn, Ge, Pb
>16	He, F, Ne	All other elements

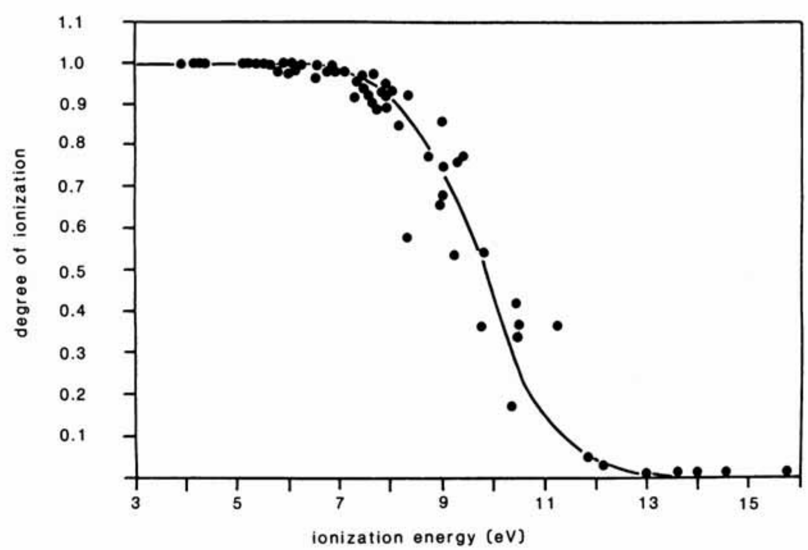

Figure 1.7 Degree of ionization α versus ionization energy for singly charged ions in the ICP. Calculated for a representative selection of 59 elements from the Saha equation, assuming values of T_i of 8000 K and n_e of 2.5×10^{15} cm^{-3}.

Sample introduction

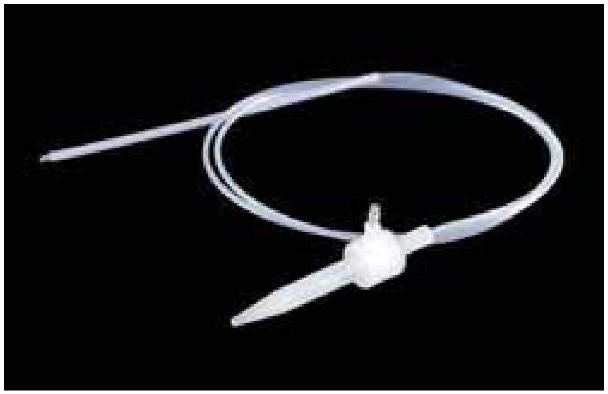

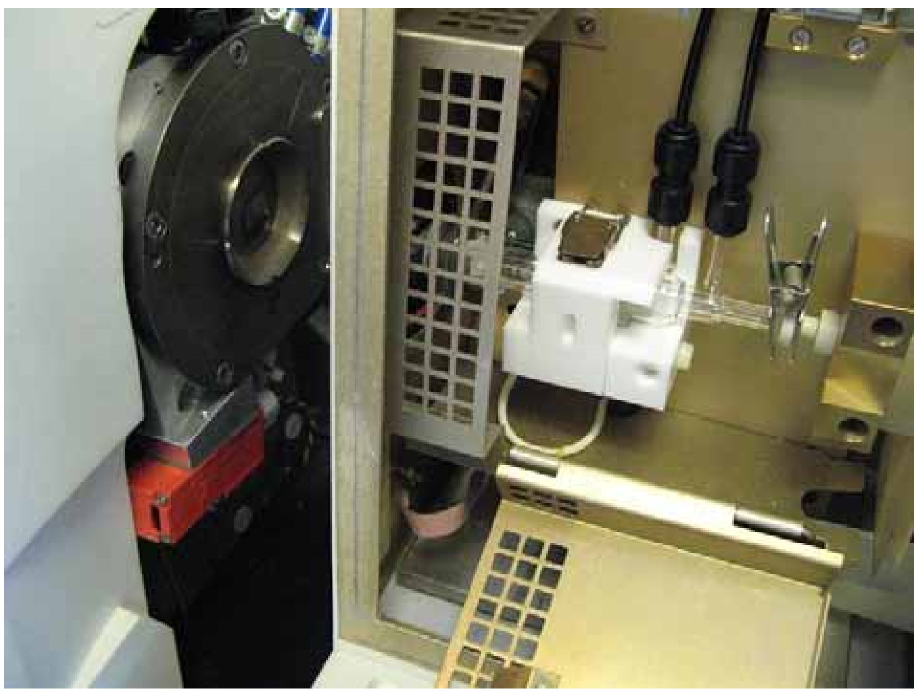

Pneumatic nebulisers

- Concentric nebulisers
- Cross-flow nebilisers

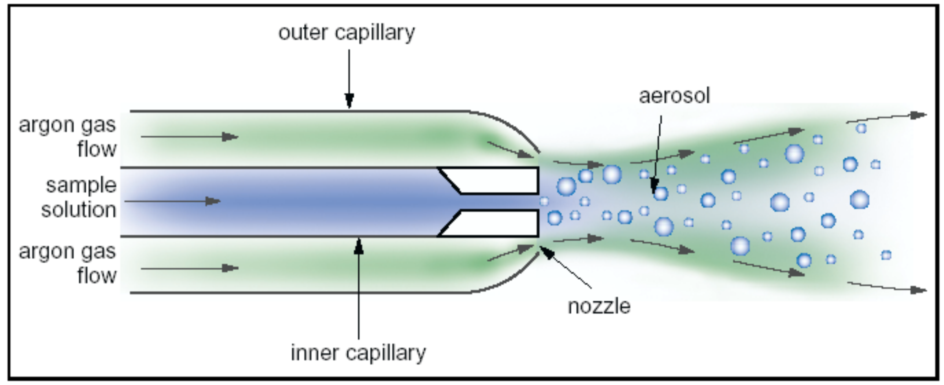

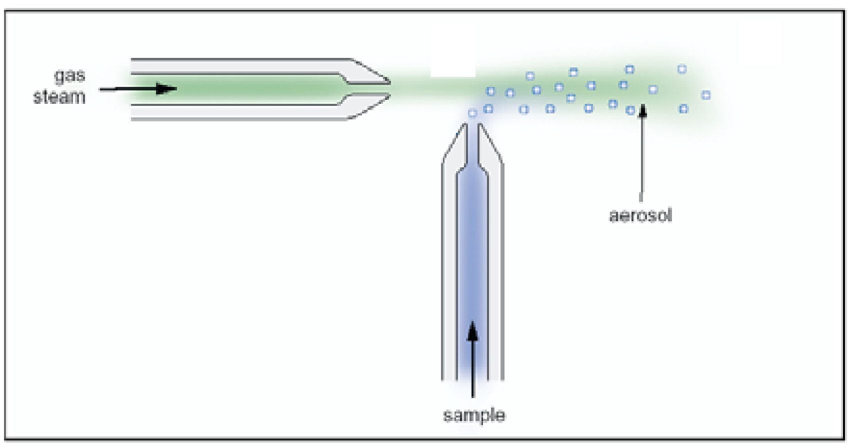

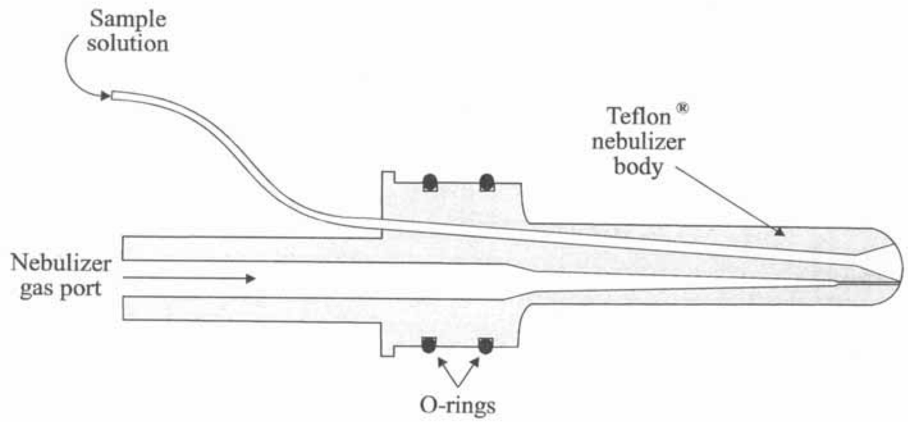

Figure 3.14 Schematic diagram of a Burgener parallel path nebulizer. (Courtesy of Burgener Research Inc.)

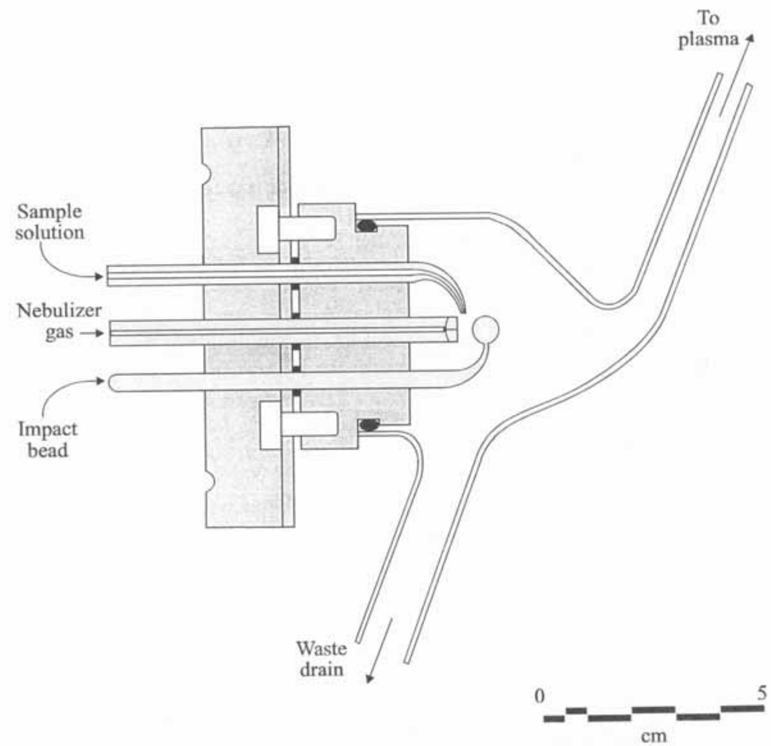

Figure 3.11 The GMK Babington nebulizer, with its glass impactor bead and spray chamber. (Courtesy of Labtam International Pty Ltd.)

The need of a spray chamber

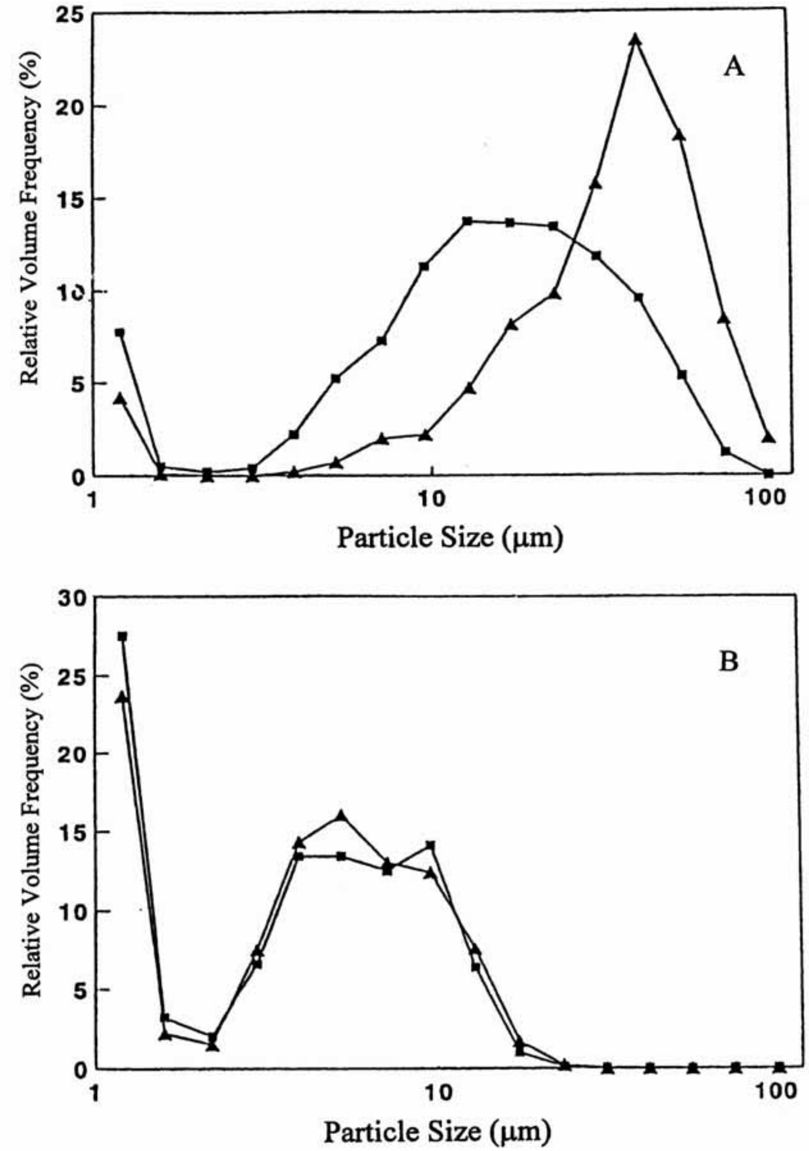

Figure 5.22 Primary and tertiary droplet size distributions for a conventional concentric nebulizer (squares) and a crossflow nebulizer (triangles) obtained with laser Fraunhofer diffraction. (A) Primary aerosol at an injector gas flow rate of 0.7 L/min. (B) Tertiary aerosol at an injector gas flow rate of 1 L/min. For both nebulizers, a double-pass spray chamber was used when the tertiary aerosol was probed. (From Reference 149, with permission.)

High efficiency nebulisers

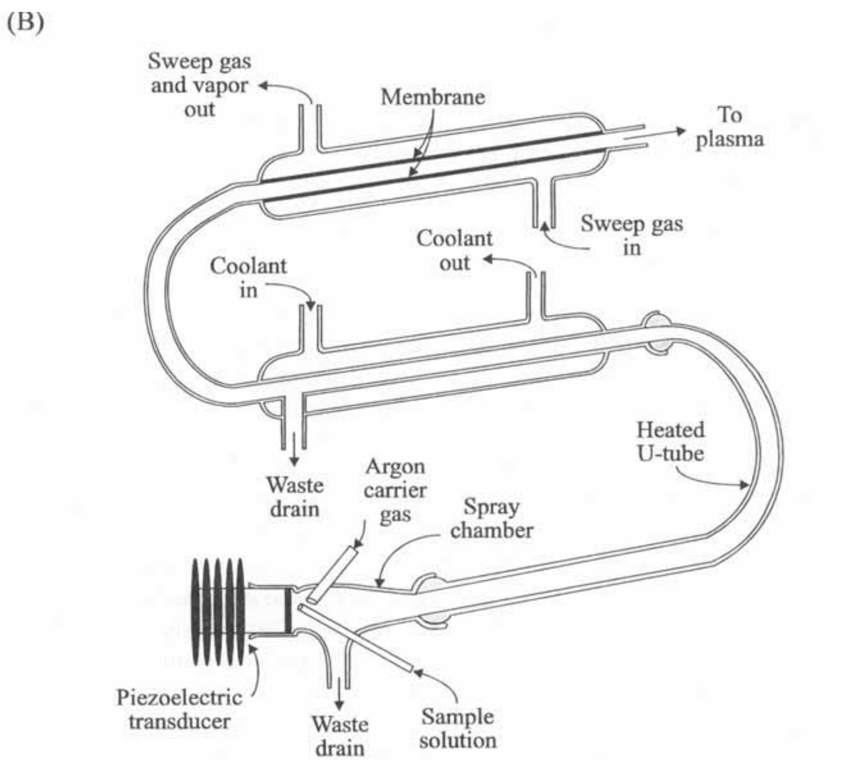

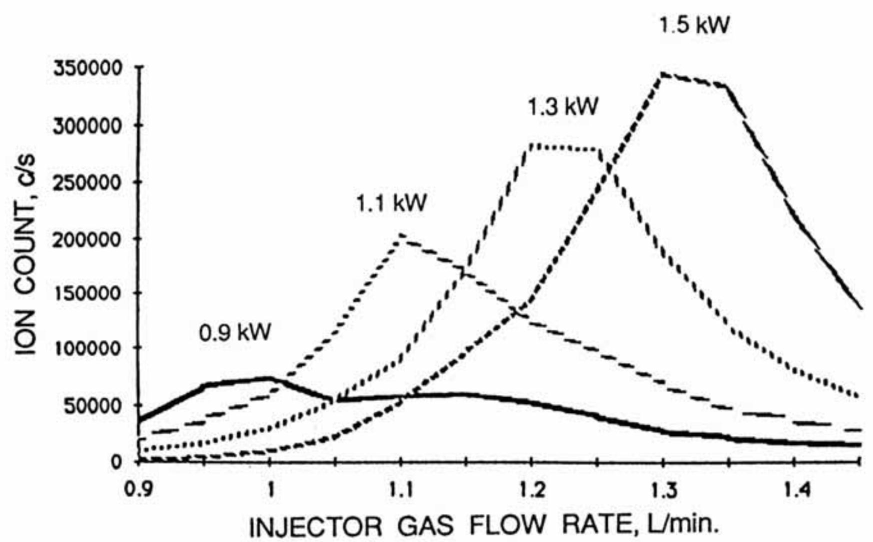

Figure 7.2 Dependence of Ga^+ signal on injector gas flow rate for a range of forward powers. (Sampling depth was 20 mm from the load coil.) (From Reference 60, with permission.)

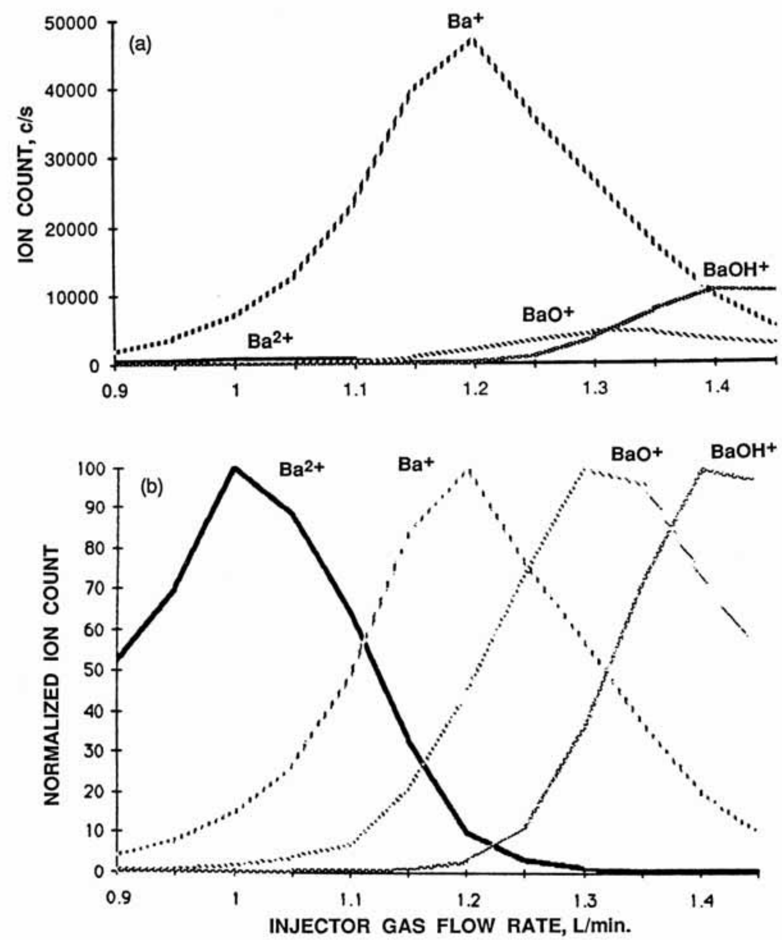

Figure 7.8 Relative (top) and normalized (bottom) plots of signal as a function of injector gas flow rate at a forward power of 1.3 kW for barium species. (From Reference 91, with permission.)

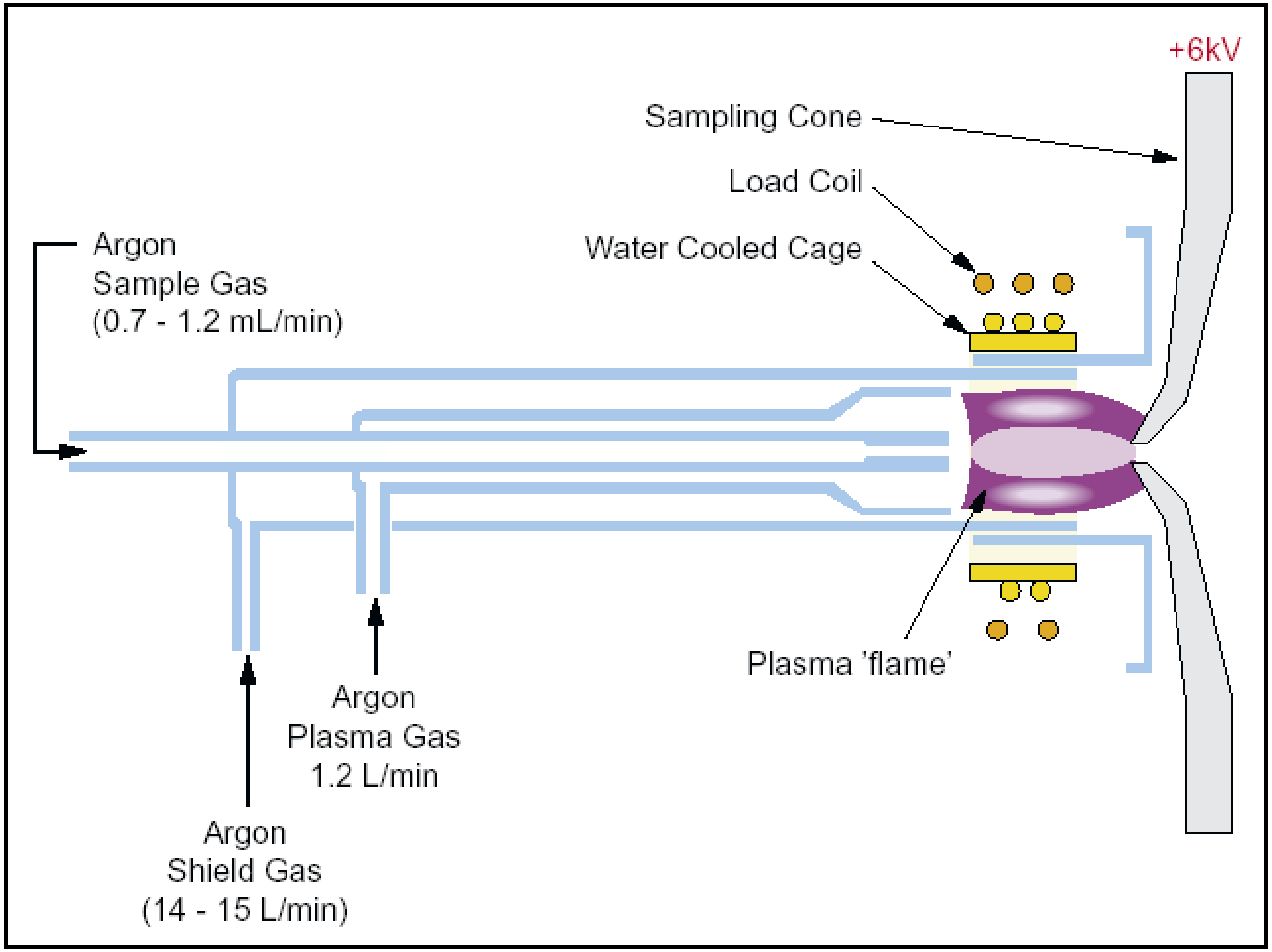
+6kV
Sampling Cone
Load Coil
Water Cooled Cage
Argon
Sample Gas
(0.7 - 1.2 mL/min)
Plasma 'flame'
Argon
Plasma Gas
1.2 L/min
Argon
Shield Gas
(14 - 15 L/min)

Pressure difference at interface region

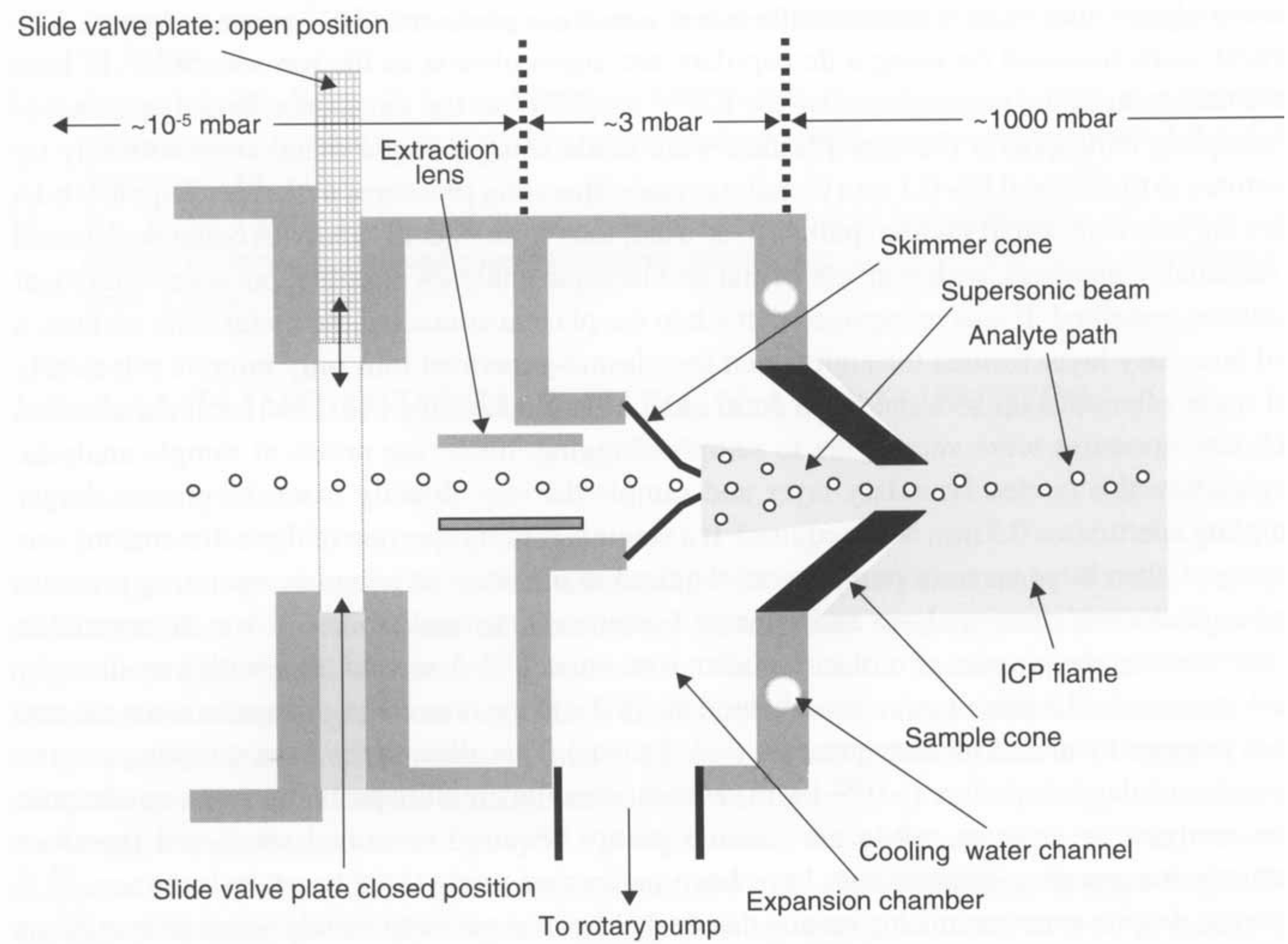

Figure 1.4 A cross section through a typical ICP-MS ion sampling interface region.

Clean samples & need for matrix removal

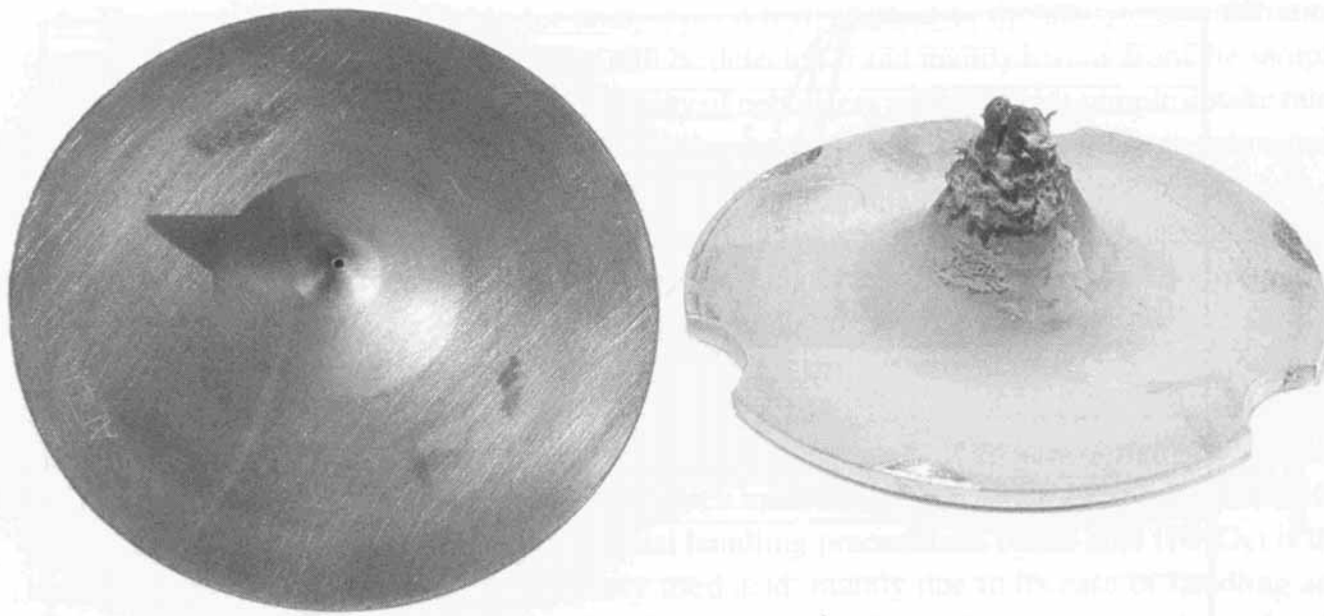

Figure 4.1 Concentrated solution of digested, freeze-dried plant material (~120 mg in ~23 mL of 2% nitric acid) leads to blockage of the cooler skimmer cone (right) while the hotter sample cone shows no deposits (left).

Mass discrimination at interface

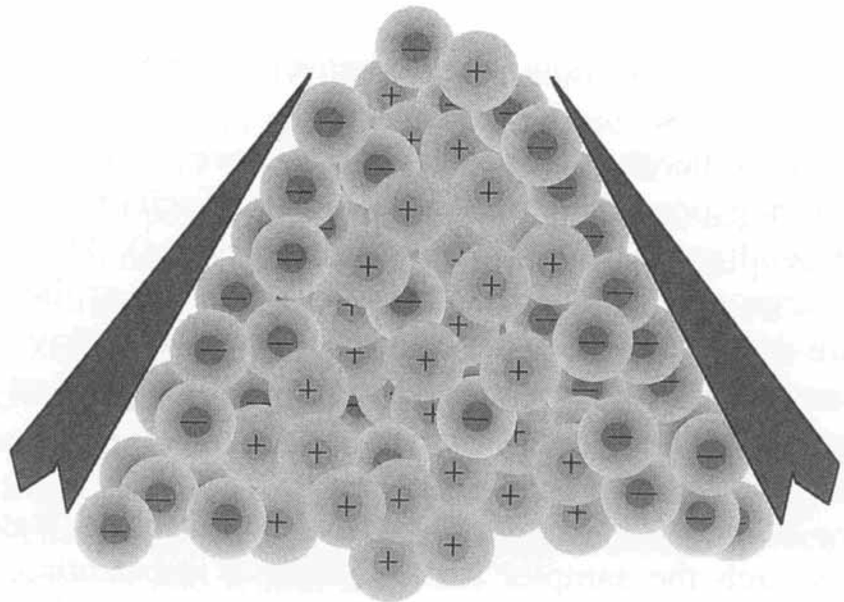

Plate 2 Under high charge density conditions, the Debye spheres of the charged particles overlap and the particles experience modified fields (they are "shielded" from the applied electrostatic field). Because of their higher mobility, electrons preferentially diffuse to the walls where an electron sheath forms. Due to the electron diffusion, a net positive charge density remains on axis and the resultant space charge field is positive. See color plate.

Detectors

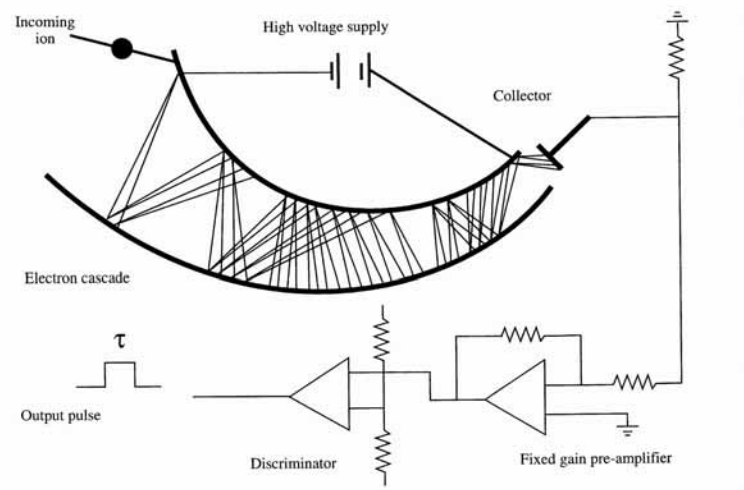

Figure 6.29 Continuous dynode electron multiplier.

Radioisotopes – focus on:

- **Sensitivity (transmission of ions to detector)**
- **Polyatomic interferences & background signals**
- **Abundance sensitivity**
- **Isotope ratios**

Alpha-spectrometry of uranium

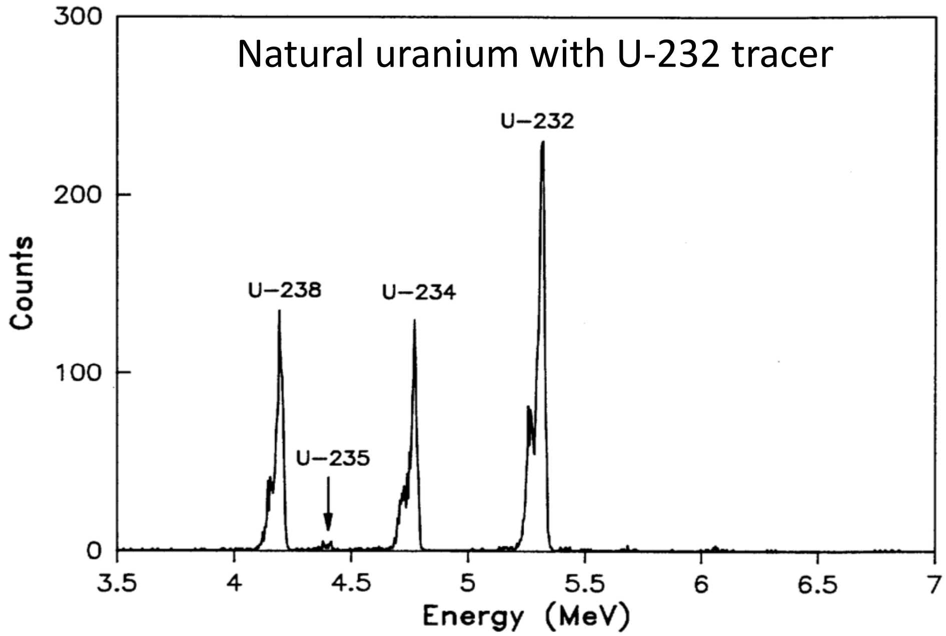

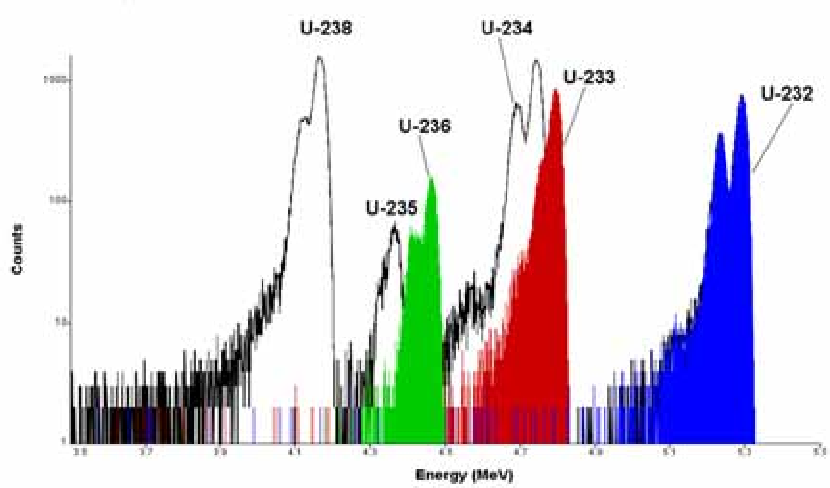

Inteference U&Th isotopes

Chemistry needed to remove matrix and interfering alpha emitters

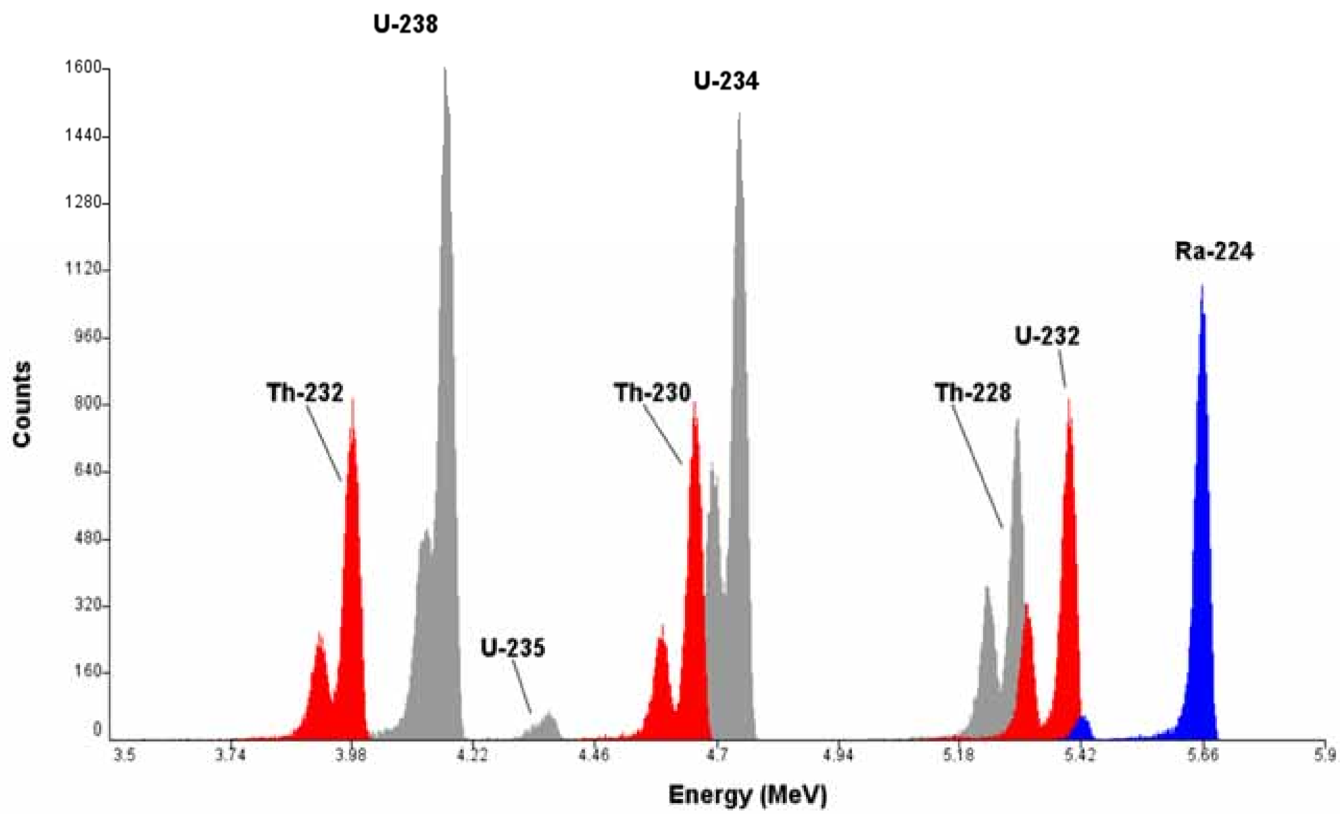

Alpha-spectra simulated by 'AASI' Monte Carlo

Alpha peak shape and the thickness of electrodeposited material

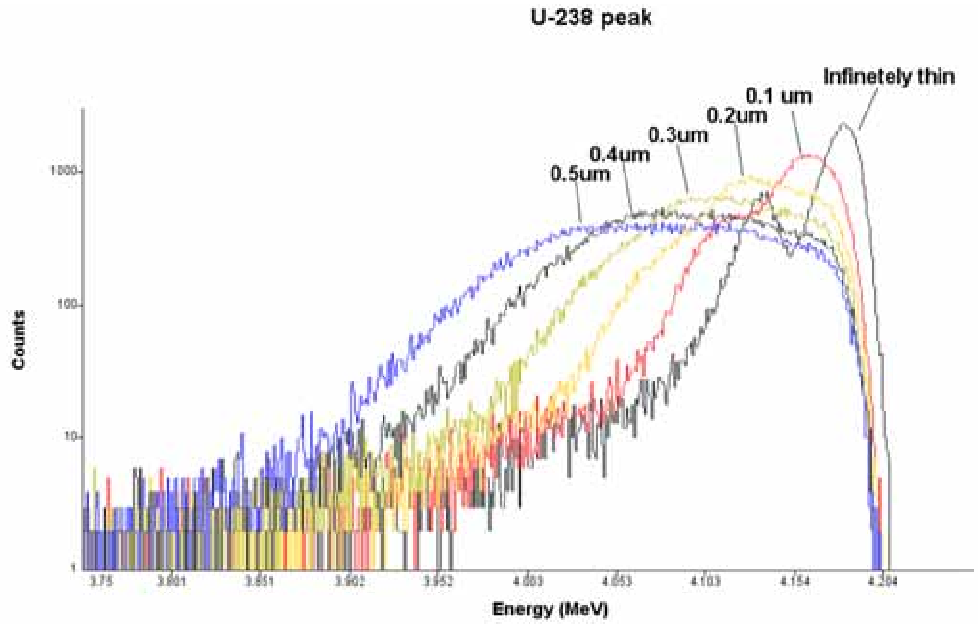

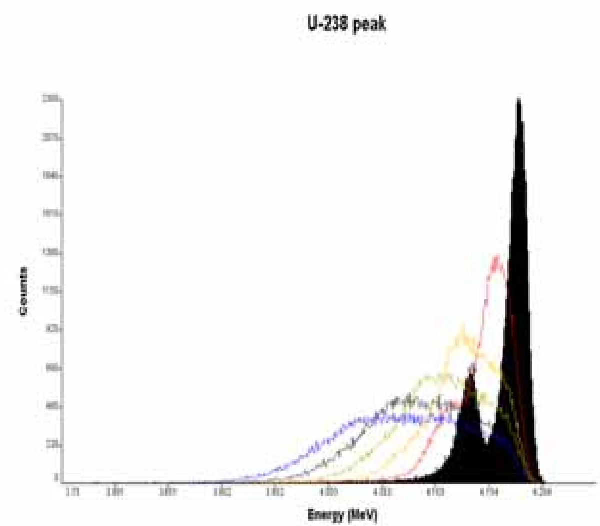

U & Th by mass - extreme ratios

(atom ratios for stable element isotopes at % levels)

	Activity ratio	Atom number ratio
$^{230}Th/^{232}Th$	0.2-5	~ 10^{-6} - 10^{-5}
$^{235}U/^{238}U$	0.045	0.0072
$^{234}U/^{238}U$	0.5-10	~ 10^{-5} - 10^{-4}

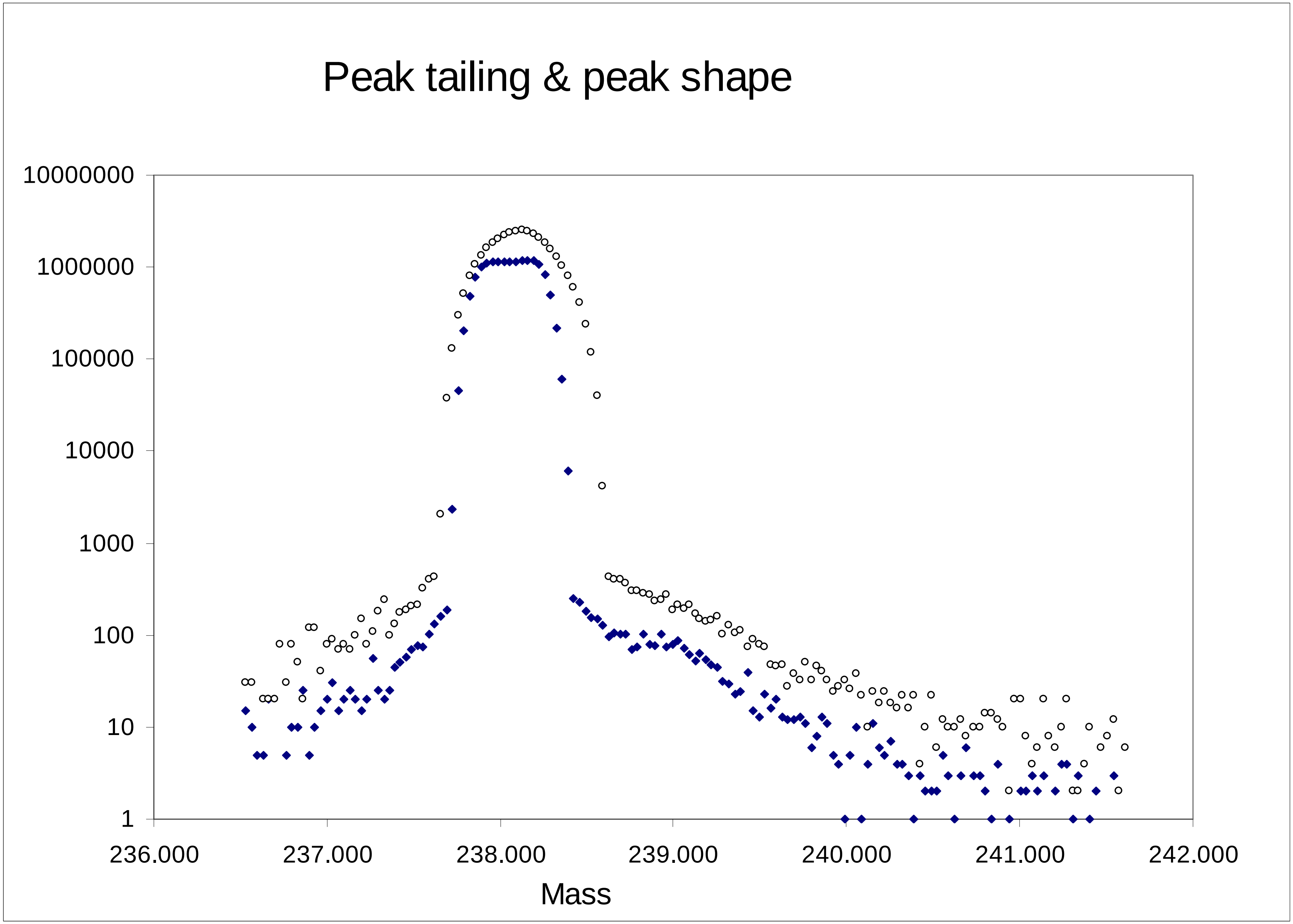

Peak tailing & peak shape
10000000
1000000
100000
10000
1000
100
10
1
236.000
237.000
238.000
239.000
240.000
241.000
242.000
Mass

Abundance sensitivity natural uranium in soil. No radiochemistry

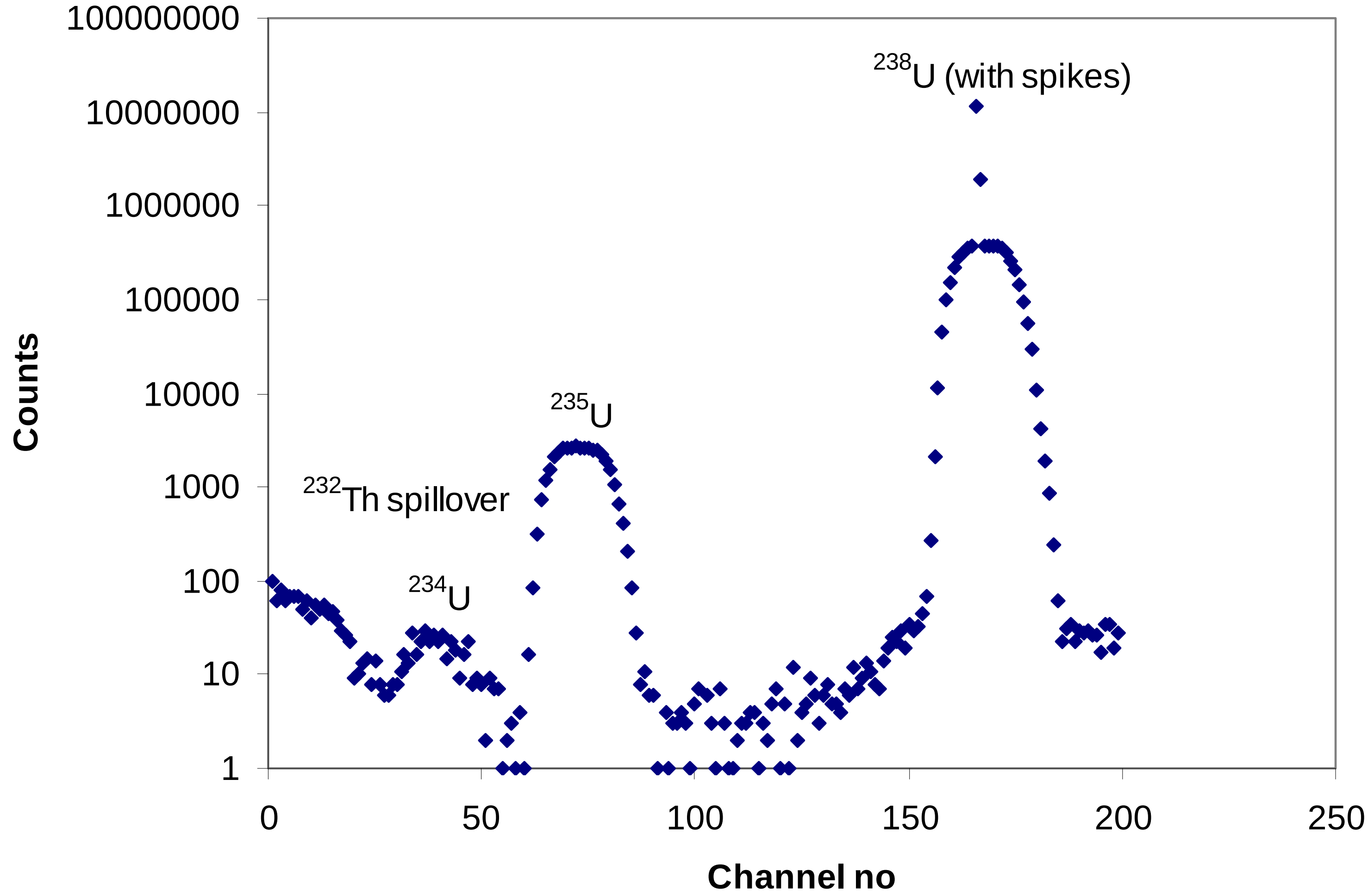

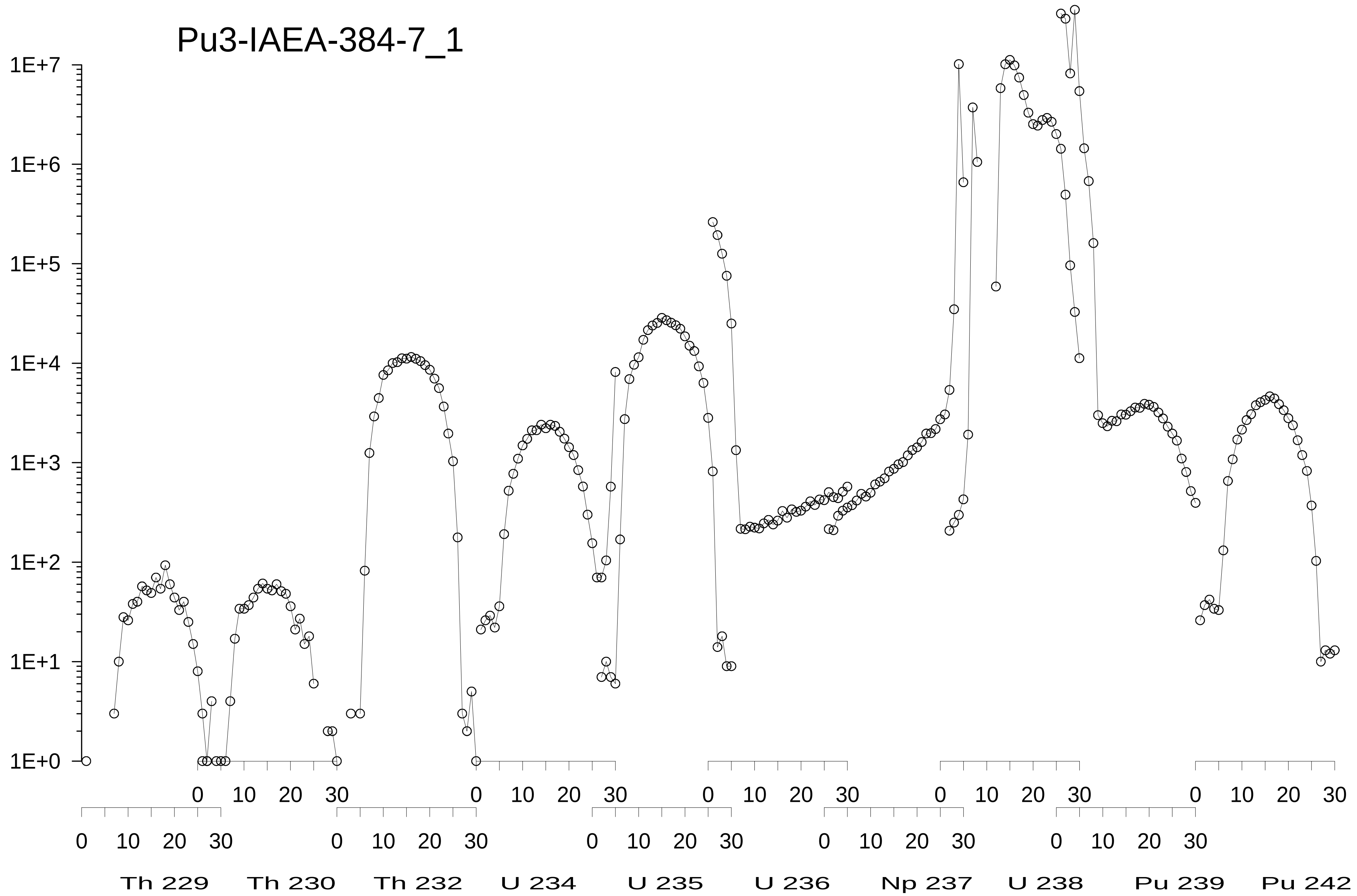

Pu3-IAEA-384-7_1
1E+7
1E+6
1E+5
1E+4
1E+3
1E+2
1E+1
1E+0
0 10 20 30
Th 229
Th 230
Th 232
U 234
U 235
U 236
Np 237
U 238
Pu 239
Pu 242

Peak shape for quadrupole MS

Rounded peak top but very little tailing

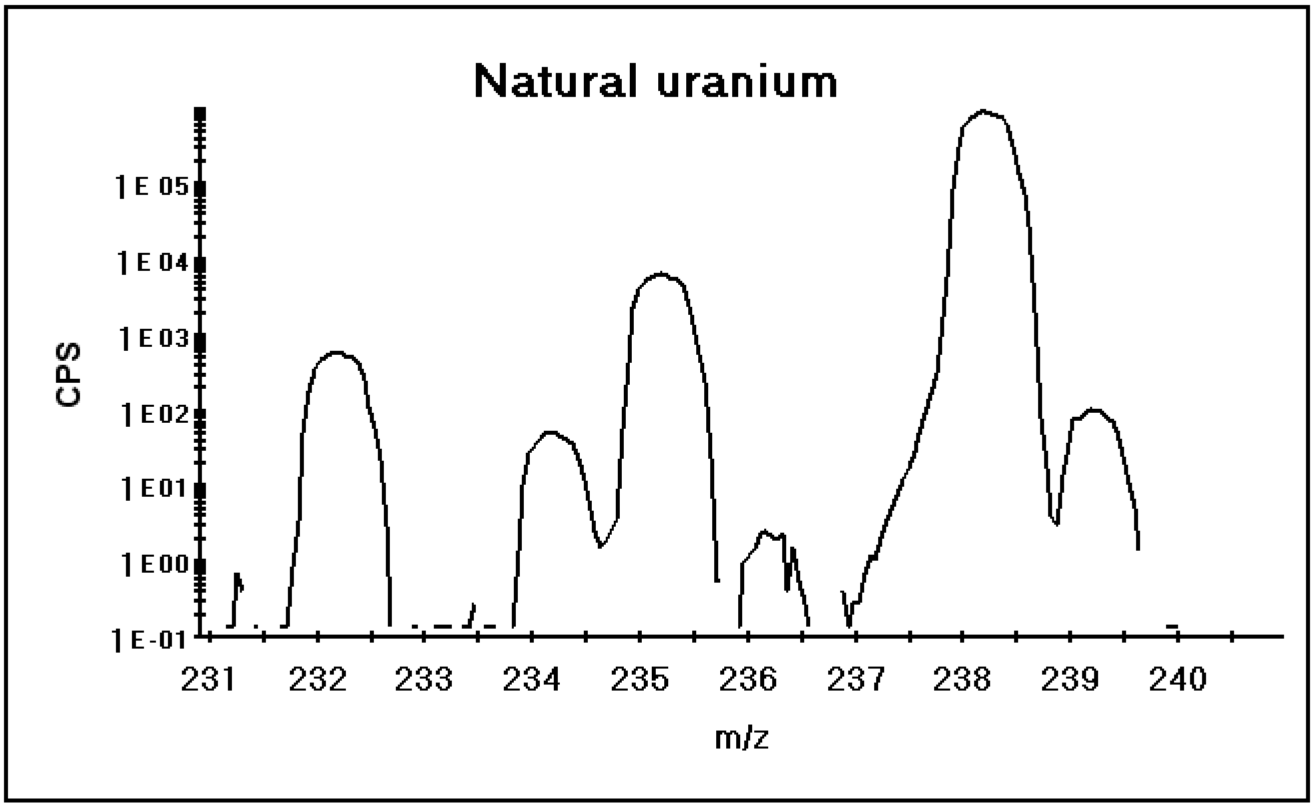

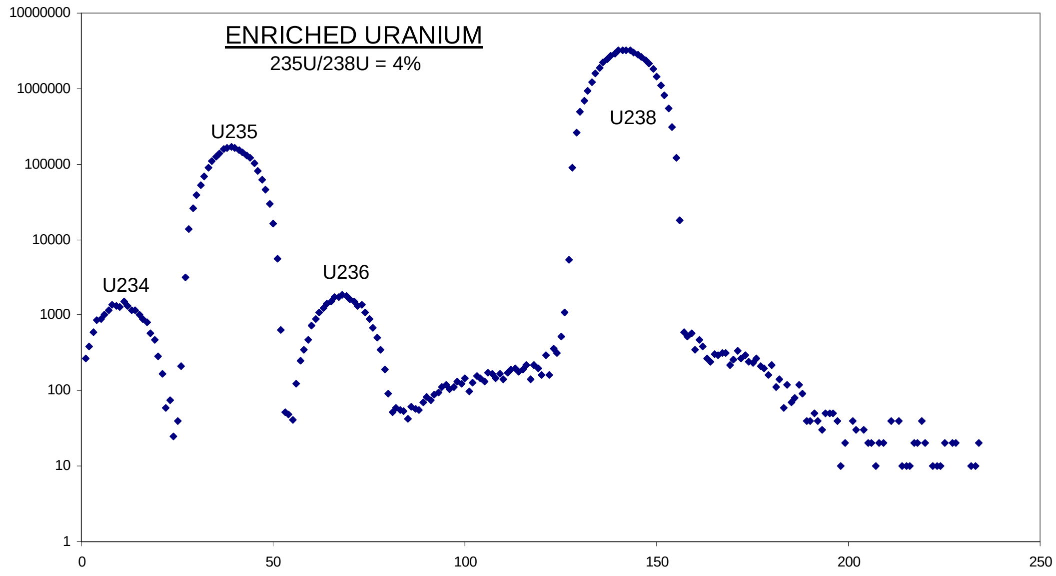
ENRICHED URANIUM
235U/238U = 4%
U234
U235
U236
U238
10000000
1000000
100000
10000
1000
100
10
1
0
50
100
150
200
250

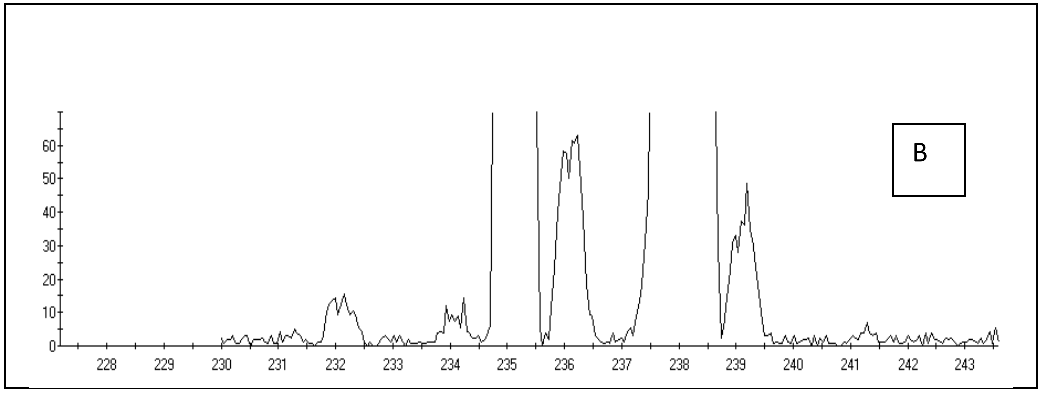
B
60
50
40
30
20
10
0
228
229
230
231
232
233
234
235
236
237
238
239
240
241
242
243

Efficiency alpha vs. ICP-MS

- **Alpha**: Geometric efficiency about 25%
- **ICP-MS**: Efficiency about 1: 10 000

- **Alpha counting** of ^{238}U (4.5 10^{9}y). One month counting $\Rightarrow$ about 10^{-12} of the sample atoms have decayed.
- **ICP-MS** measurement of ^{238}U takes about 10 minutes. 10^{-4} of sample atoms are detected.

Different separation chemistry relative to radiometric needs

Table 1
Possible interferences for Pu isotopes and required mass resolution on ICP-SFMS

Nuclide	Molecular ions	Required mass resolution, $m/\Delta m$
^{238}Pu	$^{238}U^+$	193665
	$^{206}Pb^{16}O^{14}N^1H_2^+$	3874
	$^{208}Pb^{16}O^1H_2{}^{12}C^+$	3818
	$^{208}Pb^{14}N_2{}^1H_2^+$	4654
^{239}Pu	$^{238}U^1H^+$	36885
	$^{207}Pb^{16}O^{14}N^1H_2^+$	3817
	$^{208}Pb^{16}O^{14}N^1H^+$	3430
^{240}Pu	$^{238}U^1H_2^+$	19116
	$^{208}Pb^{16}O^{14}N^1H_2^+$	3774
^{241}Pu	$^{207}Pb^{16}O_2{}^1H_2^+$	3193
^{242}Pu	$^{208}Pb^{16}O_2{}^1H_2^+$	3159
^{244}Pu	$^{206}Pb^{12}C_3{}^1H_2^+$	3293
	$^{207}Pb^{12}O_3{}^1H^+$	3031

Table 1
Possible interferences for ^{90}Sr and Pu isotopes and required mass resolution on ICP-SFMS

Nuclide	Molecular ions	Required mass resolution ($m/\Delta m$)
^{90}Sr	$^{180}W^{2+}$	1370
	$^{180}Hf^{2+}$	1372
	$^{58}Ni^{16}O_2{}^+$	2315
	$^{74}Ge^{16}O^+$	10765
	$^{52}Cr^{38}Ar^+$	19987
	$^{50}V^{40}Ar^+$	49894
	$^{54}Fe^{36}Ar^+$	155548
	$^{50}Ti^{40}Ar^+$	158287
	$^{90}Zr^+$	29877
^{239}Pu	$^{238}U^1H^+$	36885
	$^{207}Pb^{16}O^{14}N^1H_2{}^+$	3817
	$^{208}Pb^{16}O^{14}N^1H^+$	3430
^{240}Pu	$^{238}U^1H_2{}^+$	19116
	$^{208}Pb^{16}O^{14}N^1H_2{}^+$	3774

Plutonium isotopes
Interferences from clorides

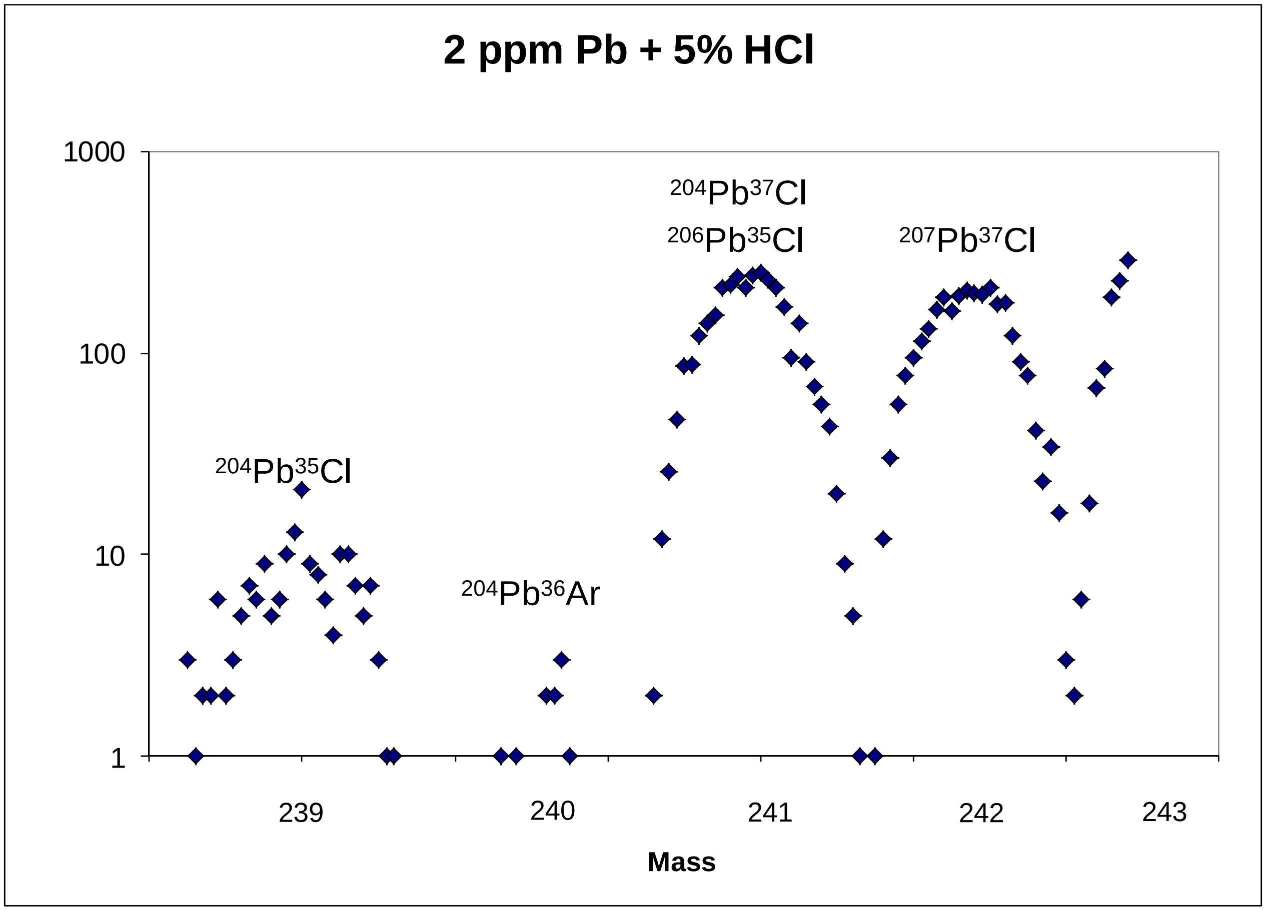

1 ppm lead and 3% HCl

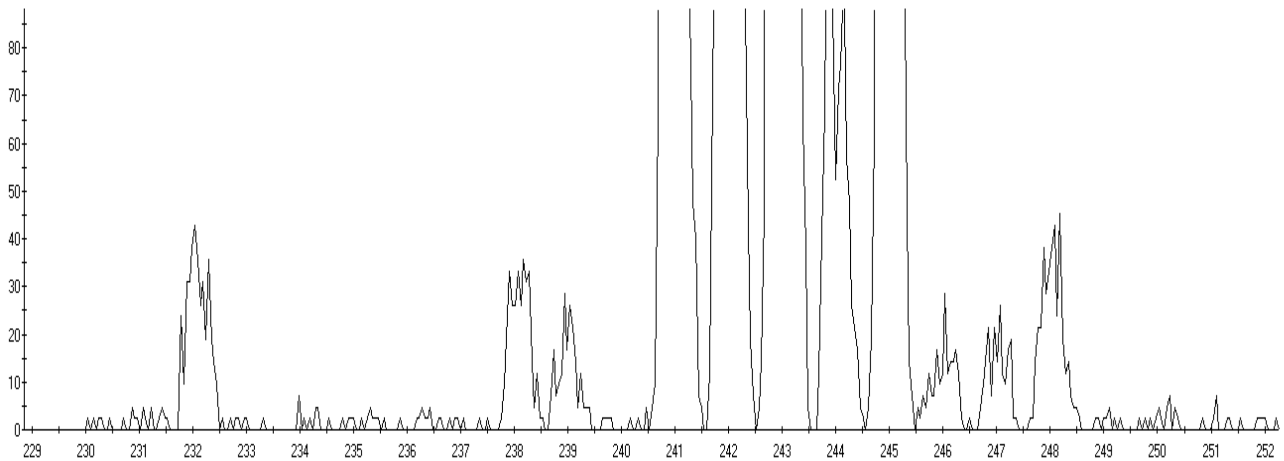

1 ppm lead and 3% HNO3

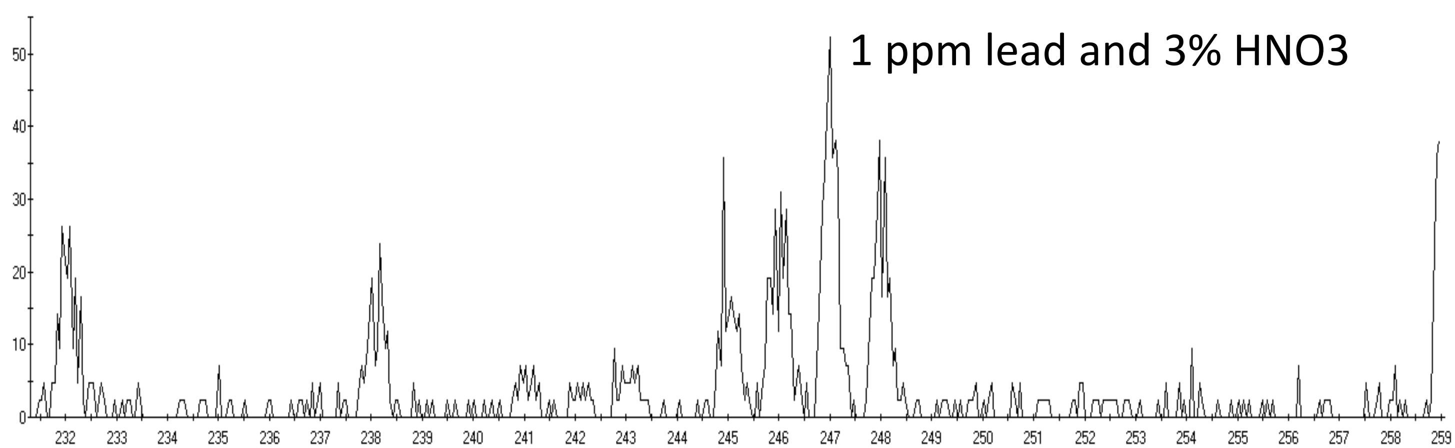

Matrix supression

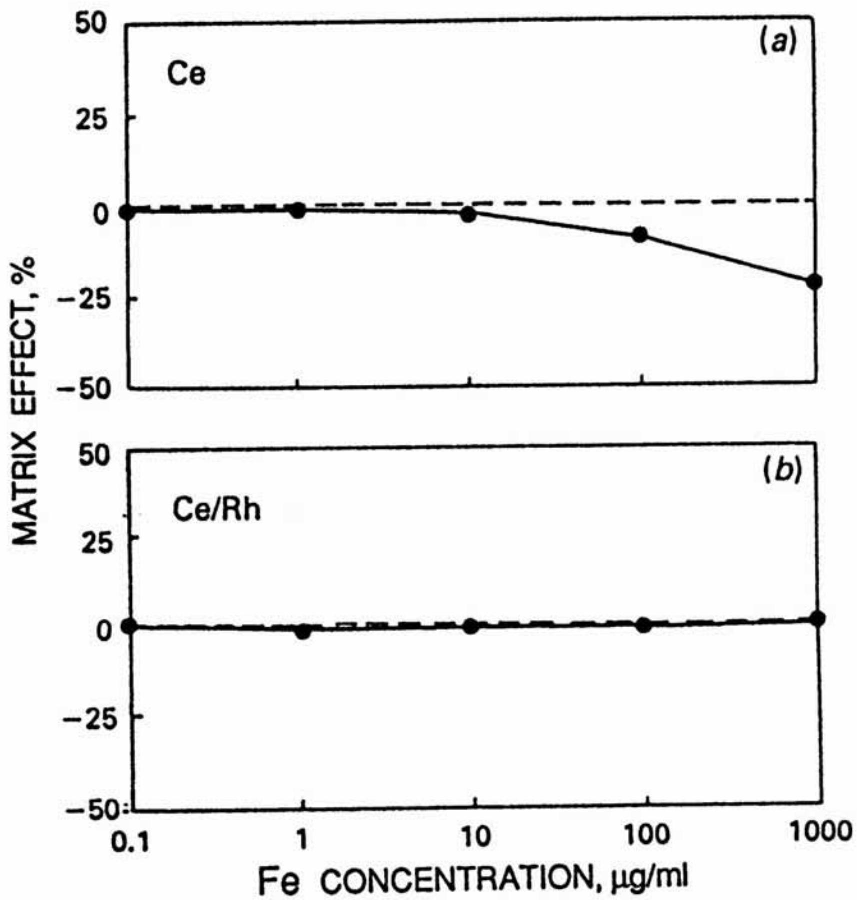

Figure 7.25 Effect of increasing Fe concentration on the Ce signal (a) with and (b) without the use of Rh as internal standard. (From Reference 294, with permission.)

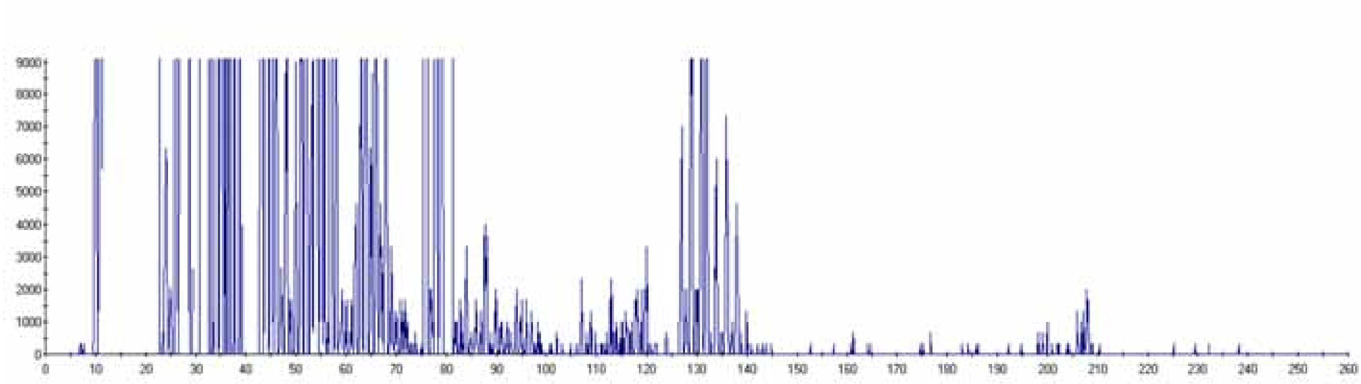

Instrument back-ground

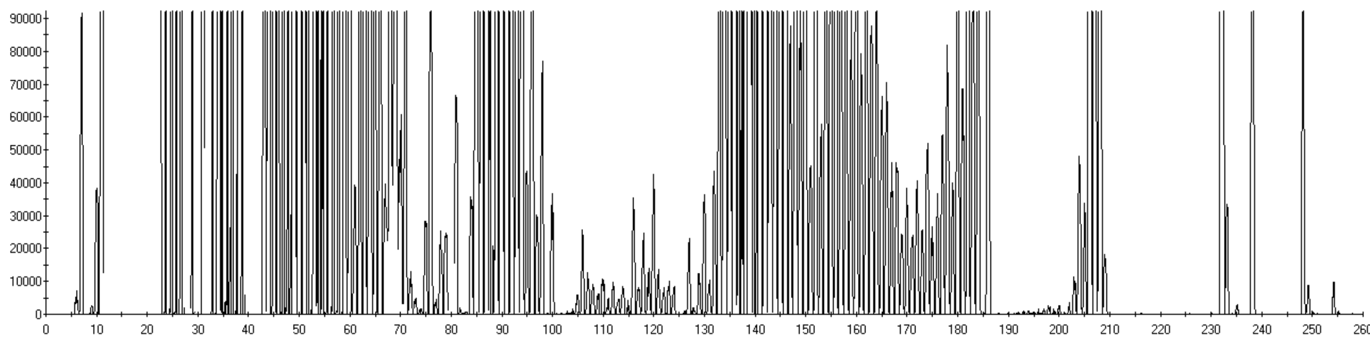

1g sediment 'raw'.

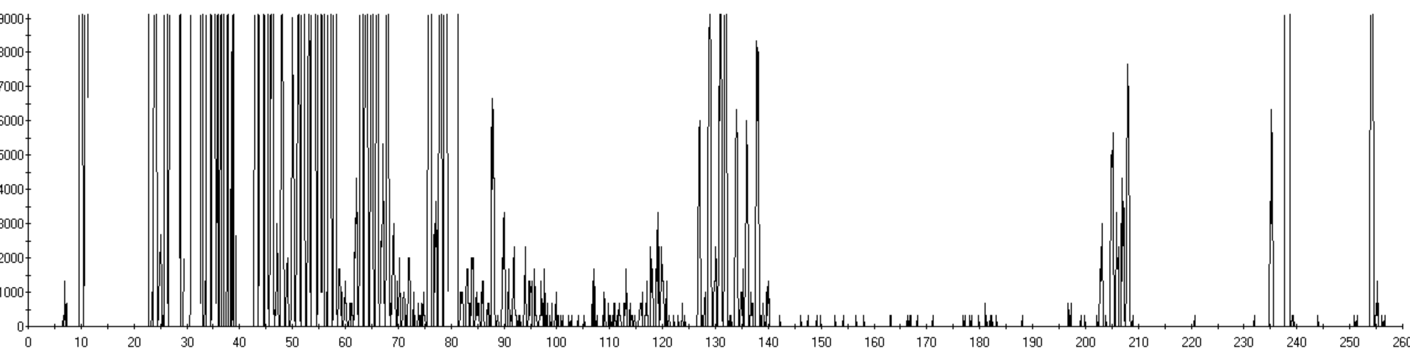

Sample after TBP-extraction

Negative side in applying chemsitry to the sample……

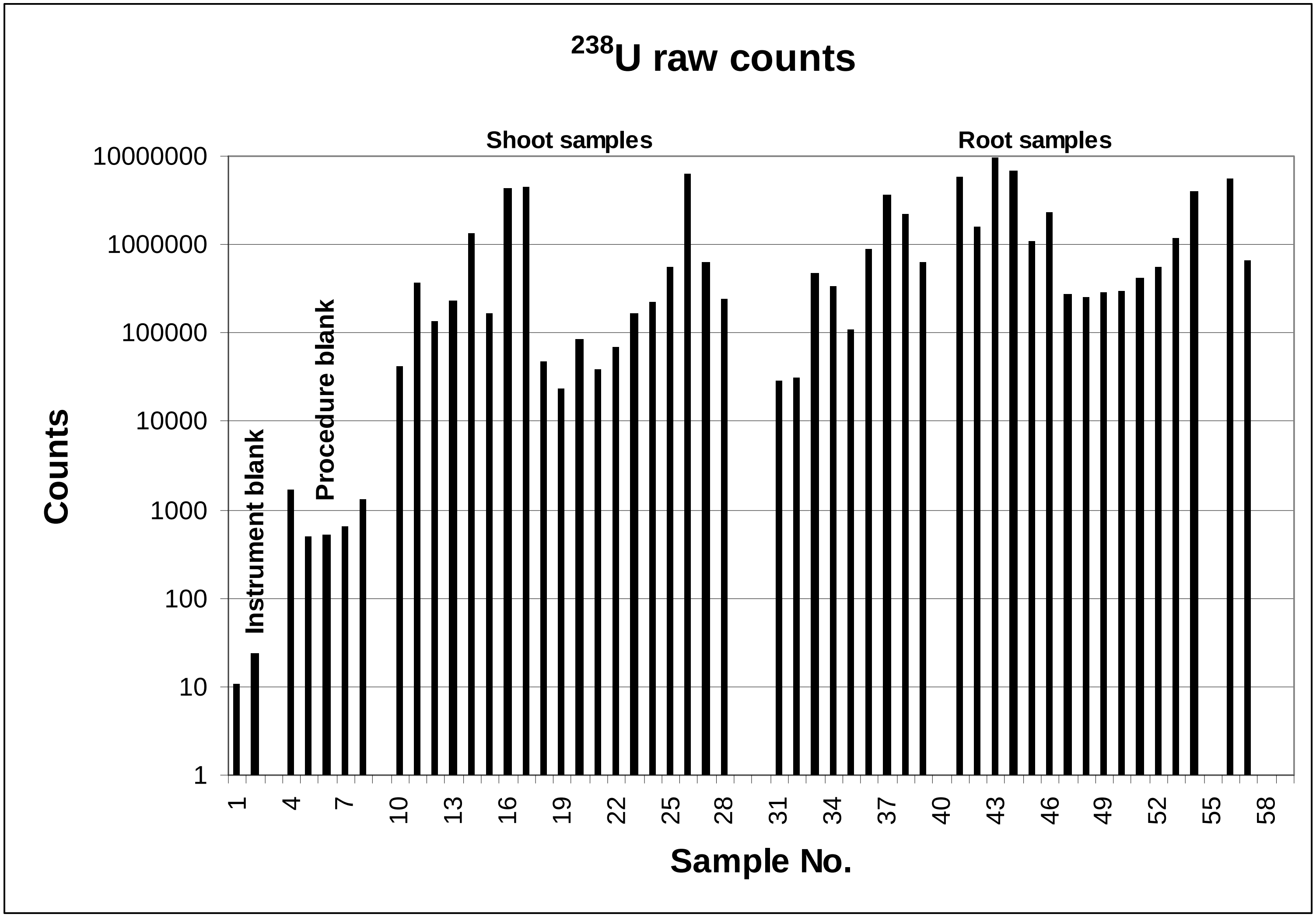

Problems in isotope ratio measurements (single collectors)

- Sample introduction system
- Plasma instability
- Dead time corrections
- Mass fractionation
- Interferences
- Abundance sensitivity (peak tailing)